

# FIRST TOLERANCE STUDIES FOR THE 4GLS FEL SOURCES

D.J. Dunning, N.R. Thompson, J.A. Clarke and D.J. Scott, ASTeC, CCLRC Daresbury Laboratory  
B.W.J. McNeil, SUPA, Department of Physics, University of Strathclyde, Glasgow, UK.

## Abstract

The Conceptual Design Report for the 4th Generation Light Source (4GLS) at Daresbury Laboratory in the UK was published in Spring 2006 [1]. 4GLS features three distinct FEL designs, each operating in a different wavelength range: an externally seeded amplifier operating in the photon energy range 8-100eV (XUV-FEL); a regenerative amplifier FEL operating over 3-10eV (VUV-FEL); an FEL oscillator operating from 2.5-200 $\mu$ m (IR-FEL). Preliminary results of tolerance studies for the FEL designs are presented. In particular, the effects of the relative timing offset between the seed pulse of the XUV-FEL and the electron bunch, as well as the effects of electron bunch timing jitter in the VUV-FEL, are presented.

## INTRODUCTION

4GLS is a 4th Generation Light Source proposed by CCLRC Daresbury Laboratory in the United Kingdom to meet the needs of the 'low photon energy' community. The 4GLS facility will combine energy recovery linac (ERL) and FEL technologies. This paper summarises the results of first tolerance studies for the XUV-FEL and the VUV-FEL. For the XUV-FEL, Genesis 1.3 [2] has been used to simulate the effects of a temporal offset between the electron bunch and the seed. For the VUV-FEL simulations, a one-dimensional, time-dependent FEL oscillator code which includes the effects of electron bunch arrival time jitter has been used.

The XUV-FEL design [3] consists of an undulator system directly seeded by a tuneable HHG laser source. It is capable of generating short, tuneable, high-brightness pulses of 8-100 eV photons with peak output powers of ~2-8 GW and typical FWHM pulse length < 50 fs. The FEL undulator consists of a lattice of undulator modules separated by beam focusing elements and diagnostics. The first eight undulator modules of the FEL will be planar, while the final five will be of APPLE-II design in order to produce variably elliptical polarised radiation.

The VUV-FEL [4] is a regenerative-amplifier-type FEL (RAFEL) [5] designed to deliver intense sub-ps pulses of tuneable coherent radiation in the photon energy range 3-10eV. A hole-outcoupled low-Q cavity using robust low reflectivity optics provides sufficient feedback to allow high gain type FEL saturation after only a few cavity round-trips. In its standard operating mode the VUV-FEL will generate temporally coherent photon beams with peak power ~500 MW and FWHM pulse lengths of ~170 fs. Cavity length adjustment may allow superradiant operation with enhanced peak powers of ~3 GW and FWHM pulse lengths of ~25 fs. These figures are the maximum values across the full wavelength range.

To enable variable polarisation, APPLE-II type undulator sections are employed throughout with a strong FODO focussing lattice and beam diagnostics distributed between sections.

## XUV-FEL SIMULATIONS

### 100 eV Pulse Amplifier Lasing

A simulation of the XUV-FEL operating at 100 eV is performed, using the CDR parameters for the case of seed/electron bunch synchronism. The full set of planar and variable undulator modules are used with the APPLE-II undulators set to helical mode so that circularly polarised radiation is generated. Figure 1 shows the seed pulse of peak power  $P = 30$  kW and duration 30 fs FWHM. Also plotted is the electron beam current of peak current  $I_{pk} = 1.5$  kA and duration 626 fs (188 $\mu$ m) FWHM.

At the end of the FEL a peak saturated power of  $P_{pk} \approx 2.4$  GW is shown in Figure 2. A 'clean' central seeded region upon a noisier pedestal is seen. The pedestal is the pre-saturation SASE - as the shot noise power is only a few tens of watts, the seed power of 30 kW saturates first.

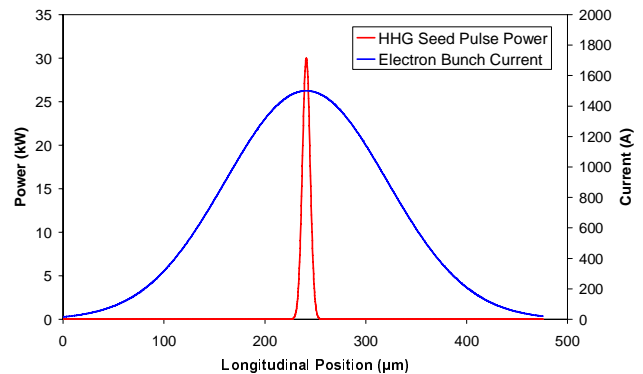


Figure 1. Input HHG seed power and electron bunch current as a function of longitudinal position.

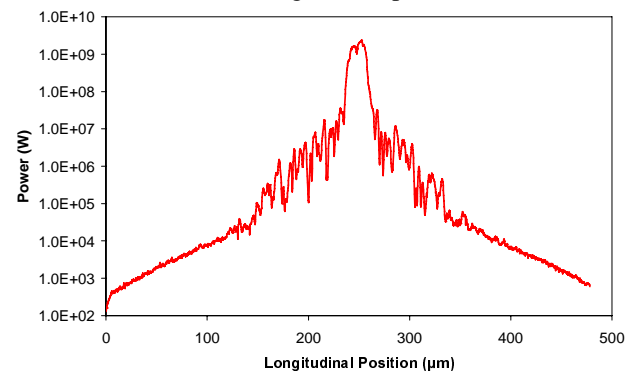


Figure 2. Radiation power at the exit of the XUV-FEL showing peak power  $P_{pk} \approx 2.4$  GW.

## 100eV Pulse Amplifier Lasing with Offset Seed

The above results are for synchronism between the peak HHG power and the peak of the electron bunch current. However, there may be an inherent noise associated with the arrival time of each bunch which results in a relative timing offset of magnitude  $\Delta t$ . Simulations have been carried out in which  $\Delta t$  is varied, as in Figure 3 (top). Also shown (bottom) is the radiation power at the end of the FEL, with the synchronous seed case for comparison. For seed offset of  $\Delta t = 100$  fs, the peak power is reduced from 2.4 GW to 1.7 GW.

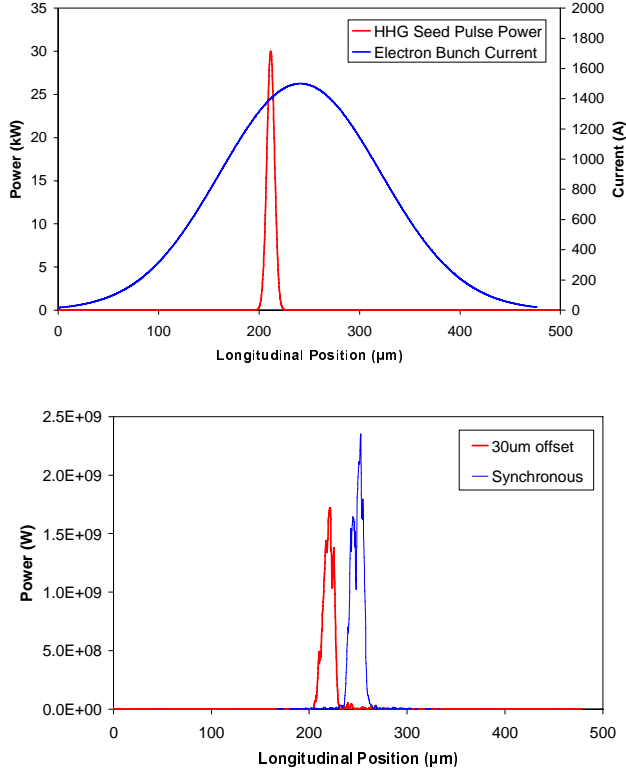


Figure 3. (Top) Seed offset by 100 fs (30  $\mu\text{m}$ ) behind the electron pulse and (bottom) radiation power at the end of the FEL for the offset case (red) and synchronous case (blue).

The offset,  $\Delta t$ , was varied between  $\pm 250$  fs and results of peak power against offset plotted in Figure 4. These results suggest that electron bunch offset should be limited to approximately  $\pm 45$  fs for peak output power to lie within 90% of the synchronous peak power  $P_{pk}$ .

From Figure 4, it is noted that the peak output power at the end of the FEL is higher for a negative  $\Delta t$  (seed pulse arriving behind the electron bunch) than for a positive offset of the same magnitude.

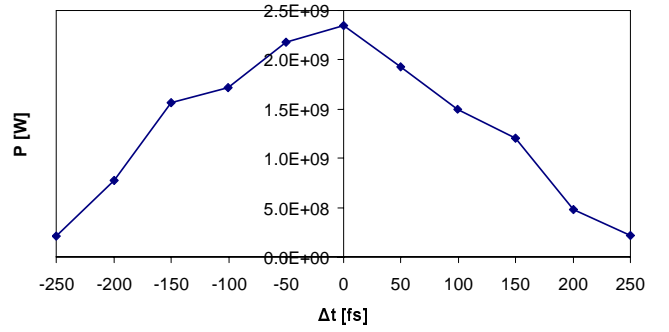


Figure 4. The effect of an offset  $\Delta t$  from electron/seed pulse synchronism upon the peak output power at the end of the FEL, for 100 eV operation.

## Comparison with FEL design formulae

The Xie design formulae [6] have been used to estimate the effects of timing offset on the saturation power. This has been done by correlating the timing offset  $\Delta t$  with the beam current via the relation:

$$I(\Delta t) = I_{pk} \exp\left(-\frac{(\Delta t)^2}{2\sigma_e^2}\right)$$

This was carried out for the planar modules only. In Figure 5 these results are compared with the results of Genesis simulations which are seen to yield a slightly more stringent restriction on  $\Delta t$ .

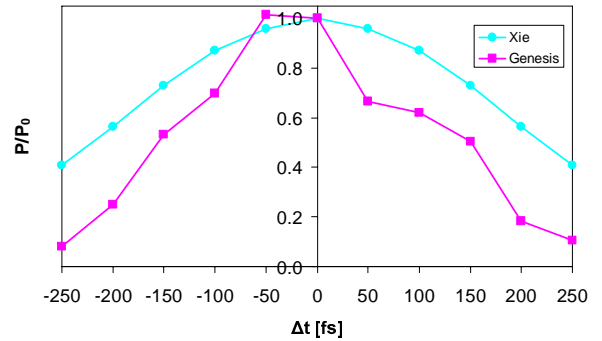


Figure 5. Simulations of the effect of an offset  $\Delta t$  from electron/seed pulse synchronism upon the peak power at the end of the FEL. The results are scaled with respect to their synchronous values at  $\Delta t = 0$ .

## VUV-FEL SIMULATIONS

A one-dimensional, time-dependent FEL oscillator code (FELO [7]) has been used. The code includes the ability to model a temporal jitter in the electron bunch arrival into the FEL cavity (this effect is simulated by adding a jitter to the cavity length).

The simulated output power and pulse width variation with cavity length detuning is shown in Figure 6 for 10eV operation in planar mode. For cavity length detuning of 18  $\mu\text{m}$ , the pulse width is at a maximum. Typical pulse shape evolution with cavity pass number is shown in Figure 7. These simulations replicate start-up from shot-

noise, with the output pulse typically developing to saturation over 10-15 passes.

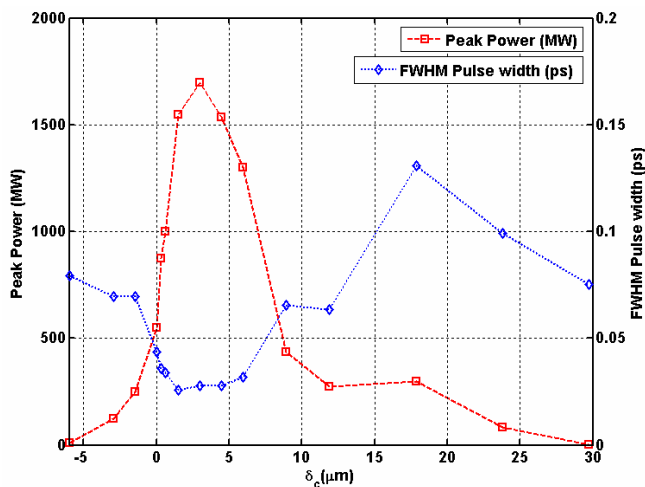


Figure 6. Plots of peak power and pulse width against cavity length detuning ( $\delta_c$ ) for simulations of the VUV-FEL operating at 10eV in planar mode.

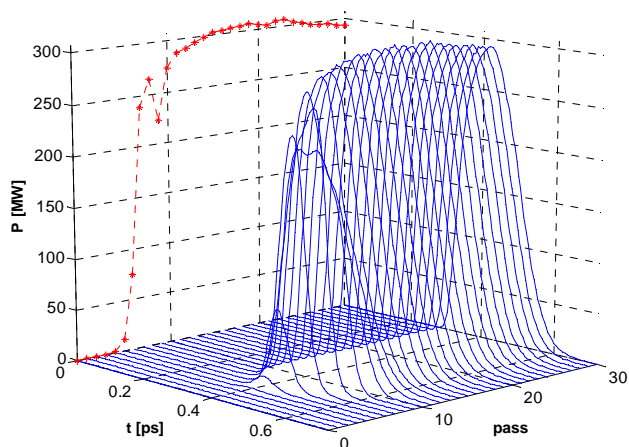


Figure 7. FEL simulation of the VUV-FEL at 10eV and cavity length detuning of  $18\mu\text{m}$  with zero electron bunch arrival time jitter. The red points show the peak intensity of the pulse at each pass.

### Simulations with Electron Bunch Time Jitter

In Figure 8 the variation of pulse shapes for different cavity pass numbers are plotted for three different electron bunch arrival time jitter values. Increasing jitter shows increasing variation of the pulse shape with pass number. The pulse shape remains approximately Gaussian for the cases where jitter  $\leq \pm 80$  fs. For the greater jitter value of  $\pm 120$  fs, the output pulse is seen to have a less stable shape.

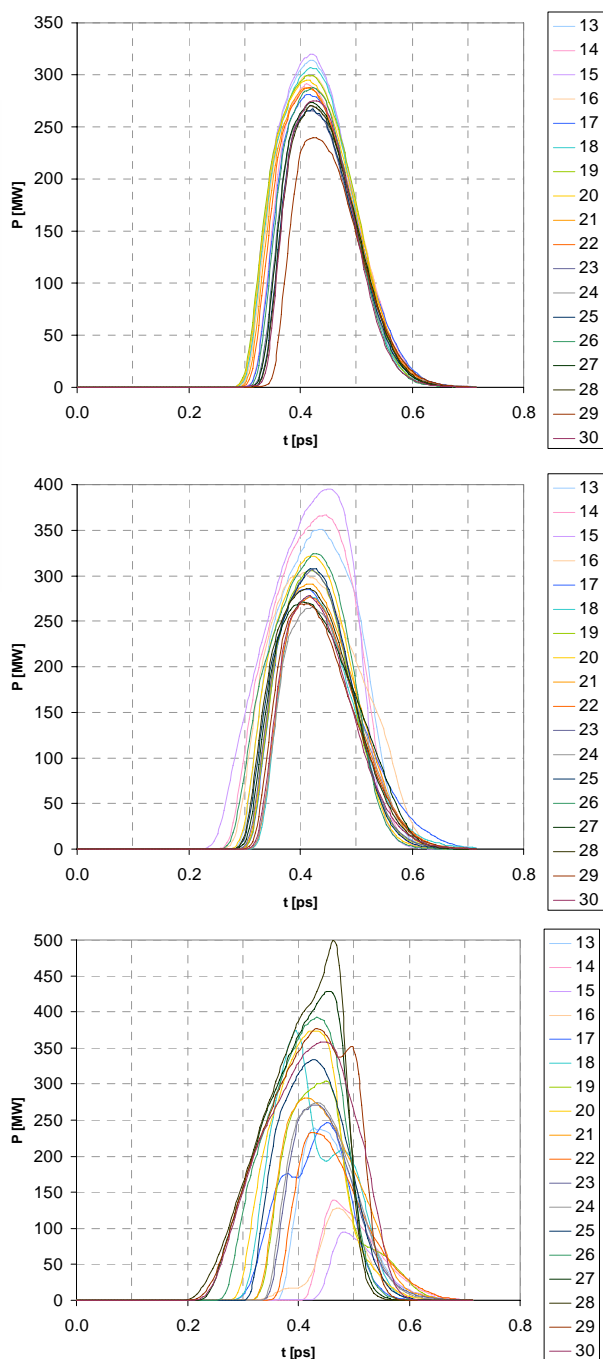


Figure 8. Variation of pulse shape with cavity pass number for electron bunch arrival time jitters of  $\pm 40$  fs (top),  $\pm 80$ fs (middle) and  $\pm 120$  fs (bottom). Only passes 13 to 30 are shown. Increasing the temporal jitter shows increasing variation of the pulse shape.

### Analysis of output power

Due to shot noise, repeat runs from the same input data yield slight variations in output. For jitter = 0, five runs were carried out and an average peak power was plotted as shown in Figure 9.

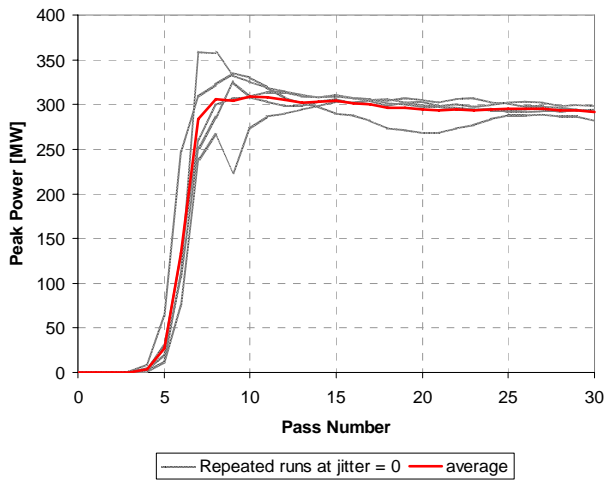


Figure 9. Peak power of pulse with pass for repeated runs at jitter = 0. The variation between different runs is due to the effect of shot noise only.

Repeated runs were carried out for different jitter values and the RMS variations from this average (at saturation) were calculated and are presented in Table 1.

Table 1. Variation of saturation power for different values of electron bunch arrival time jitter.

Jitter (fs)	Saturation Power (MW)
$\pm 0.0$	$300 \pm 2.5\%$
$\pm 20$	$300 \pm 4.1\%$
$\pm 40$	$300 \pm 6.0\%$
$\pm 80$	$300 \pm 8.0\%$
$\pm 120$	$300 \pm 18.8\%$

For the case of maximum jitter where the pulse shape remains approximately Gaussian (jitter =  $\pm 80$  fs), the output power at saturation is  $\sim 300\text{MW} \pm 8\%$ . The evolution of pulse shape with pass is shown for jitter of  $\pm 80$  fs in Figure 10.

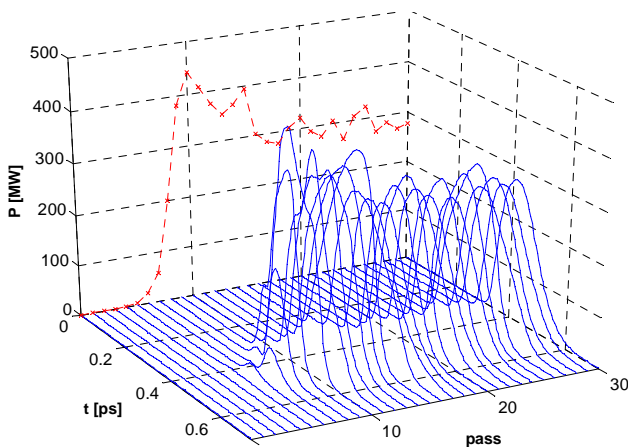


Figure 10. FELo simulation of the VUV-FEL at 10eV for cavity length detuning of  $18\mu\text{m}$  with jitter of  $\pm 80$  fs. The red points show the peak intensity of the pulse at each pass.

### Short-pulse operation of the VUV-FEL

For a cavity length detuning of  $1.5\mu\text{m}$ , operation is in superradiant mode, peak output power is near maximum and the pulse width is at a minimum (see Figure 6). Simulations using the FELo code show that at this cavity length detuning, it is possible for the side-spikes to develop into the peak with maximum power [8]. The evolution of the pulse where electron bunch arrival time jitter =  $\pm 40$  fs is shown in Figure 11.

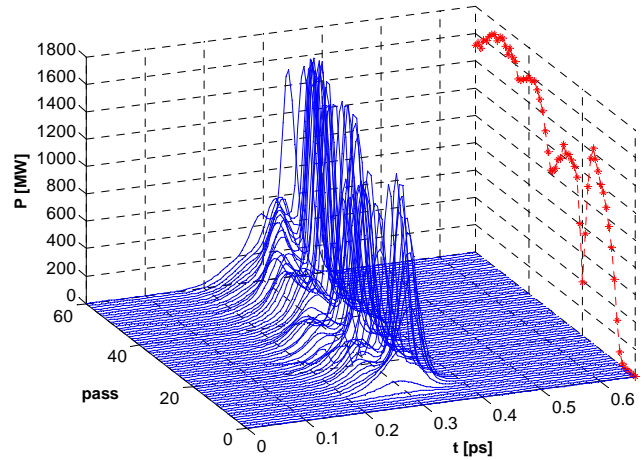


Figure 11. Pulse shape evolution for short-pulse operation with electron bunch arrival time jitter of  $\pm 40$  fs.

### CONCLUSION

First tolerance studies for the 4GLS XUV-FEL and VUV-FEL have been carried out. For the XUV-FEL, increased offset between seed and electron pulse has been shown to decrease saturation power. For the VUV-FEL electron bunch arrival time jitter has been shown to result in increased instability in the shape of the output optical pulse. It has been concluded that for the XUV-FEL, temporal electron bunch offset should be limited to approximately  $\pm 45$  fs for output power to be within 90% of optimum. For the VUV-FEL, jitter should be limited to approximately  $\pm 80$  fs for approximate Gaussian output with peak power within  $\pm 8\%$  of optimum.

### REFERENCES

- [1] 4GLS Conceptual Design Report, Council for the Central Laboratory of the Research Councils, UK (2006), available from: <http://www.4gls.ac.uk/documents.htm#CDR>
- [2] S. Reiche, Nucl. Inst. Meth. Phys. Res. A, 429, 243, (1999)
- [3] B.W.J. McNeil et al, 'The Conceptual Design of the 4GLS XUV-FEL', these proc.
- [4] N.R. Thompson et al, 'A 3D Model of the 4GLS VUV-FEL Conceptual Design Including Improved Modelling of the Optical Feedback Cavity', these proc.
- [5] B. W. J. McNeil, IEEE J. of Quantum Electron., 26, 1124 (1990)
- [6] Ming Xie, Proc of 1995 Part. Accel. Conf., (1996) p183.
- [7] B.W.J. McNeil et al, 'FELo, a one dimensional time-dependent FEL oscillator code', these proc.
- [8] D.J. Dunning, 'Results of simulations varying the electron bunch arrival time jitter for the 4GLS VUV-FEL', Internal Report fgls-upcdr-rpt-0013, 2006.